

Evaluation of earthquake ground motion and site effects in the Thessaloniki urban area by 3D finite-fault numerical simulations

Chiara Smerzini¹ · Kyriazis Pitilakis¹ · Kiana Hashemi²

Received: 26 January 2016 / Accepted: 26 July 2016 / Published online: 8 August 2016
© Springer Science+Business Media Dordrecht 2016

Abstract In this study earthquake ground motion in the Thessaloniki urban area is evaluated using a 3D spectral element numerical approach. The availability of detailed geotechnical/geophysical data from past microzonation studies together with the seismological information regarding the relevant fault sources allowed for the creation of a large-scale 3D numerical model. The latter is suitable for generating finite-fault physics-based ground shaking scenarios within the city of Thessaloniki up to maximum frequencies of about 1.5 Hz. As a representative case study, the simulation of the historical M_W 6.5 June 20th 1978 Volvi earthquake is addressed. The results show that reasonable estimates can be obtained in terms both of ground motion time histories at the only available strong motion station and of spatial distribution of peak ground motion parameters, as compared to the regional map of macroseismic intensity and to the predictions of attenuation laws. The numerical model is, then, used to provide insights into 3D site effects occurring in the city of Thessaloniki, by showing the comparison between synthetic and experimental Standard Spectral Ratios (SSR) as well as the effect of non-linear visco-elastic soil behavior and the spatial variability of amplification factors with respect to outcrop bedrock basement. The results of this study demonstrate the potentialities of 3D physics-based numerical modeling for deterministic-based seismic hazard assessment studies in large urban areas characterized by complex geological configurations, such as the Thessaloniki area.

✉ Chiara Smerzini
chiara.smerzini@gmail.com

Kyriazis Pitilakis
kpitilak@civil.auth.gr

Kiana Hashemi
seyedehkiana.hashemydahaj@polimi.it

¹ Department of Civil Engineering, Aristotle University of Thessaloniki, P.O. B. 424, 54124 Thessaloniki, Greece

² Department of Civil and Environmental Engineering, Politecnico di Milano, Piazza Leonardo da Vinci 32, Milan, Italy

Keywords 3D numerical modeling · Seismic wave propagation · Earthquake ground motion · Site effects

1 Introduction

Thessaloniki, the second largest city in Greece after Athens, is located in the Axios-Vardar zone, which is adjacent to the Servomacedonian massif (see Fig. 1), extending from the FYrom-Bulgaria border up to the North Aegean Trough. The Servomacedonian massif is one of the most seismotectonically active zones in Europe; a large portion of its seismicity is associated with the Mygdonia graben, around 25 km northeast of Thessaloniki, where on June 20th 1978 a destructive earthquake with moment magnitude $M_W = 6.5$ occurred. The 1978 earthquake, also referred to as Volvi earthquake from the lake of the same name, caused extensive damage to many villages located close to the epicentral area (Stivos, Scholari, Peristeronas, Gerakarou), as well as in Thessaloniki, where the death toll reached the value of 45 people (Roumelioti et al. 2007).

The 1978 Volvi earthquake is considered as the first earthquake with a serious impact on a big modern urban center like the city of Thessaloniki (Papazachos et al. 1979). As a matter of fact, the earthquake attracted the attention of many researchers and marked the

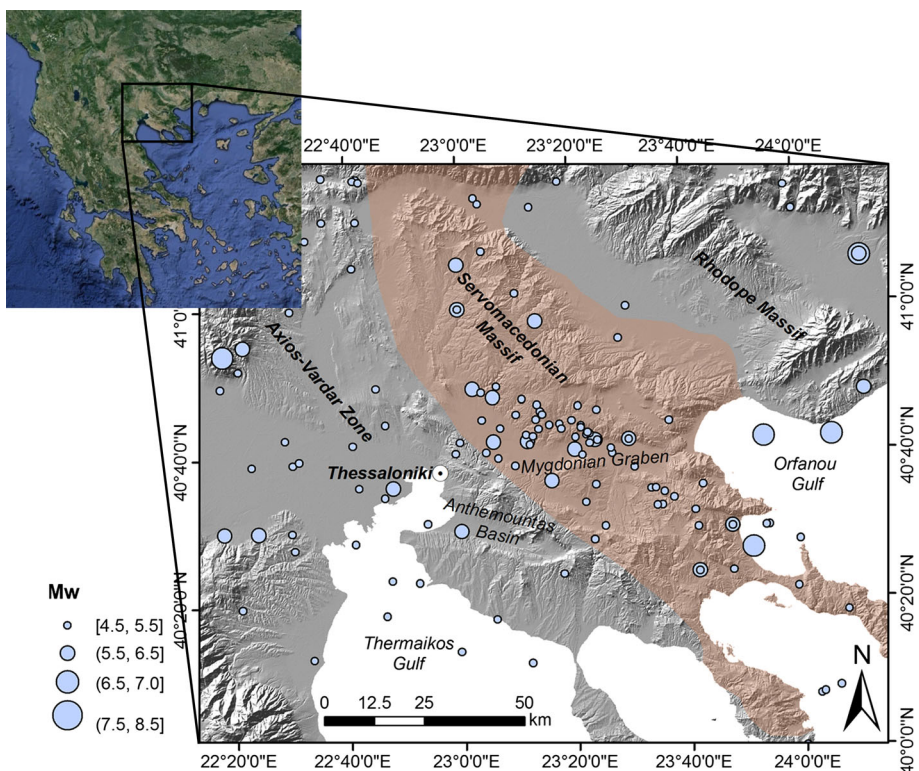


Fig. 1 Map of the broader area of Central-Northern Greece with indication of the main geologic zones. The catalog of known earthquakes with magnitude greater than 4.5 for the period 550 B.C. (before Christ)-2010 is shown (from Papazachos et al. 2000, 2010)

beginning of several studies, extending from the analysis of the seismological features of the 1978 seismic sequence as well as of the broader Thessaloniki area (see thorough overview in Roumelioti et al. 2007), up to microzonation studies and researches related to the quantification of local site effects (e.g., Lachet et al. 1996; Triantafyllidis et al. 2004a, b; Raptakis et al. 2004a, b; Ptilakis 2010; Ptilakis et al. 2015) and to the construction of 2D/3D geotechnical/geophysical models for the Thessaloniki subsurface structure (Anastasiadis et al. 2001; Apostolidis et al. 2004; Raptakis and Makra 2010). In addition to these seismological and geotechnical studies, inventories of the building stock, the electric power network, the water supply system and the road network were developed for seismic risk assessment applications (e.g. Argyroudis et al. 2014).

This series of investigations has led to a thorough characterization of the Thessaloniki urban area from a geologic, geotechnical/geophysical and structural/lifeline engineering point of view. For this reason, the city has been selected as a benchmark site in the framework of different research projects funded by the European Commission (2004–2007 LESSLOSS FP6 European Integrated Project; 2009–2012 SYNER-G FP7 European Collaborative Research Project; on-going 2013–2016 STREST FP7 European Collaborative Research Project), which have stimulated further improvements and analyses.

Given this deep knowledge, the main aim of this work was to carry out a numerical study on the prediction of earthquake ground motion in the Thessaloniki urban area, based on a full 3D model both of the seismic fault rupture and of the source-to-site propagation path, with reference, in particular, to the M_w 6.5 1978 earthquake. The availability of extensive geotechnical and geophysical data together with the seismological information regarding the fault sources having a strong impact on the city allowed for the set-up of a large-scale 3D computational model by spectral elements. The latter is suitable for predicting physics-based earthquake scenarios in the region of Thessaloniki, preserving the full spatial coherence of wavefield from the source up to the site. The first efforts to study 3D seismic wave propagation effects within the Thessaloniki urban area at a wide scale were made by Skarlatoudis et al. (2010, 2011, 2012), who adopted a finite-difference numerical approach. Compared to these studies, the modeling presented in this paper takes into account finite-fault ruptures rather than point sources and, therefore, it is more suitable to study source-related effects, which may be very significant in the near-field region. Although the simulation of the 1978 Volvi earthquake is mainly addressed in this paper, the 3D model is not limited to this event but it can be easily used for the simulation of different seismic rupture scenarios from sources located in the proximity of the city of Thessaloniki.

In recent years, physics-based numerical simulations of earthquake ground motion including a full 3D seismic wave propagation model from the extended seismic source (modeled either kinematically or dynamically), through heterogeneous Earth media, up to localized topographic and/or geologic irregularities (e.g. alluvial basins), have gained an increasing attention worldwide (see e.g. overview of recent advances in 3D physics-based numerical simulations in Paolucci et al. 2014 and impressive applications in USA such as the CyberShake project, Graves et al. 2011, and the ShakeOut scenario, Porter et al. 2011). Several numerical techniques are available, based on Finite Differences (Graves 1996; Pitarka 1999), Finite Elements (Bielak et al. 2005), and Spectral Elements (Faccioli et al. 1997; Komatitsch and Vilotte 1998). In this work, numerical simulations were performed using an innovative high-performance code, namely SPEED (Mazzieri et al. 2013), based on the Discontinuous Galerkin Spectral Elements Method (DGSEM).

The paper is organized as follows. First, the seismotectonic and geologic context of the study area is illustrated in Sect. 2. After presenting the code, SPEED, used for the 3D

numerical analyses, along with its parallel performance on the super-computing machines of the Aristotle University of Thessaloniki (Sect. 3), the main features of the computational model are addressed in Sect. 4. Section 5 presents the simulation of the June 20th 1978 earthquake, focusing on the comparison between synthetics and observations and the generation of ground shaking maps at regional scale. Finally, insights into the evaluation of 3D site amplification effects and of their spatial variability within the Thessaloniki urban area are provided in Sect. 6, with emphasis on the comparison between predicted and observed Standard Spectral Ratios (SSRs), the effect of soil non-linearity and the computation of amplification factors.

2 Seismotectonic and geologic context

The broader Thessaloniki area lies in Central Macedonia, an area characterized by extensive North-West (NW)–South-East (SE) and East (E)–West (W)-trending continental-type basins and grabens, filled with Neogene and Quaternary sediments. They formed as a result of Miocene to present extensive brittle extensional deformation that mainly related to high-angle normal faults (Tranos et al. 2003). Among them, the Mygdonian graben is the largest basin in the area (see Fig. 1) and its continuous seismic activity poses a serious threat to the city of Thessaloniki.

The tectonic regime of the broader area is characterized by extensional deformation associated mostly with NW–SE, NE–SW, E–W and NNE–SSW trending faults (Tranos et al. 2003; Paradisopoulou et al. 2006). The E–W striking faults are mainly normal dip-slip, while the NW–SW and ENE–WSW ones occasionally show strike-slip components of movement. The fault system bounding the southern boundaries of the Mygdonia graben (Gerakarou fault) was responsible of the destructive 1978 earthquake.

Figure 2 points out the main seismic sources of the broader Thessaloniki area (with particular reference to the region modeled in this work), as provided by the Greek Database of Seismogenic Sources (GreDaSS: <http://gredass.unife.it/>; Caputo et al. 2012), a repository of geological, tectonic and active fault data for the Greek territory, together with the epicenters of the historical events with $M_W > 6$. Epicenter location and magnitude of the historical events are taken from Papazachos et al. (2000, 2010) and from Roumelioti et al. (2007), specifically for the 1978 Volvi earthquake. The boundaries of the computational model, described in the following sections, are also indicated, as denoted by the super-imposed blue box.

In the study area historical seismicity reveals the occurrence of moderate to large earthquakes, associated mainly with the Mygdonia Basin and the Anthemountas faults, with magnitude up to $M_W = 6.5$ from historical to present times. In particular, three distinct periods of high seismicity near the city can be identified: (1) 7th century, characterized by two main events in 677 ($M_W = 6.4$) and 700 ($M_W = 6.5$); (2) 15th–18th century, with two major earthquakes in 1677 ($M_W = 6.2$) and June 22th 1759 ($M_W = 6.5$) in the Anthemountas region (south of Thessaloniki); (3) 20th century, with two destructive earthquakes, both with $M_W = 6.5$, occurring on July 5th 1902 and June 20th 1978 along the EW Mygdonia graben.

From a geological point of view, the Thessaloniki urban area is characterized by three main geological “macro” structures oriented in the NW–SE direction. Starting from the deepest one, these formations can be summarized as follows:

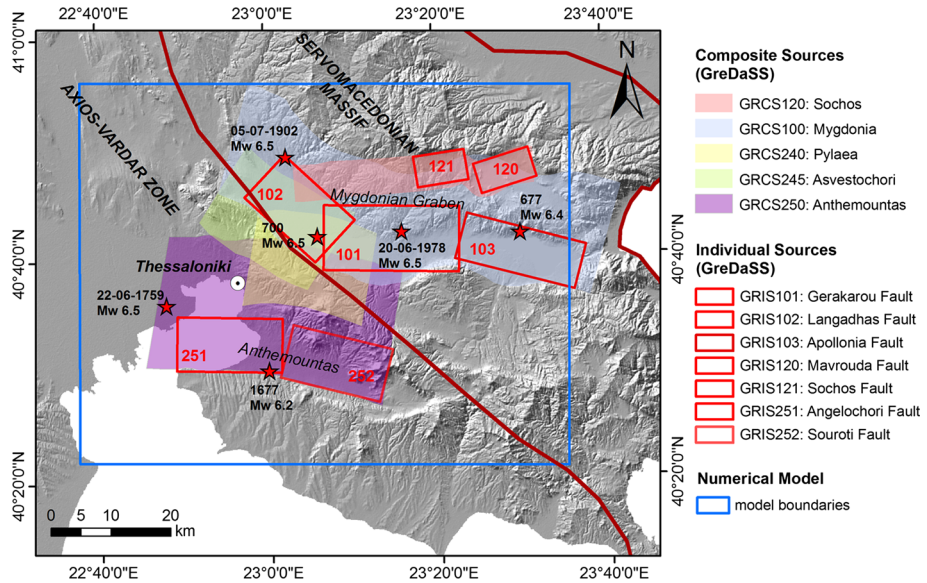


Fig. 2 Map of the main seismogenic sources (from GreDASS database: GRCS = GReek Composite Source; GRIS = GReek Individual Sources, i.e. faults) and of the epicenters (denoted by the stars) of historical earthquakes with $M_w > 6$ in the broader Thessaloniki area. The boundaries of the SPEED model are also superimposed (blue box)

- metamorphic substratum consisting of crystalline rocks (gneiss, epigneiss and green shists), which outcrops at the N-NE border of the city and reaches a depth larger than 500 m near the coastline in the W-WS direction;
- sedimentary deposits, mainly of Neogene period, dominated by the stiff red silty clays, covering the bedrock basement beneath the city;
- recent generally soft deposits consisting of clays, sands and pebbles of Holocene period.

The definition of 3D thematic maps of these geological formations together with their geotechnical/geophysical characterization was addressed, first, by Anastasiadis et al. (2001) and, subsequently, by Apostolidis et al. (2004). Anastasiadis et al. (2001) presented the results of a detailed geophysical and geotechnical survey undertaken in the framework of a microzonation study limited to the urban area of Thessaloniki. The main outcome of this work was the publication of a comprehensive set of 1D profiles, 2D cross-sections and 3D thematic maps of seven soil formations identified within the city, apt for seismic site response analyses. Apostolidis et al. (2004) estimated 1D shear wave (V_s) profiles up to a depth of about 300 m at 16 sites in the broader area of Thessaloniki, applying the spatial autocorrelation coefficient method (SPAC) to array measurements of microtremors. Combining these new data with the geotechnical maps from Anastasiadis et al. (2001), the authors identified five soil formations and proposed updated 3D thematic maps of the geotechnical/geophysical model applicable to the urban area of Thessaloniki. In this work, the model by Apostolidis et al. (2004) has been adopted.

3 The numerical simulation method: SPEED

The numerical simulations presented in this paper have been carried out by the open-source software package SPEED (*SP*ectral *E*lement in *E*lastodynamics with *D*iscontinuous *G*alerkin), jointly developed by the Laboratory for Modeling and Scientific Computing (MOX) of the Department of Mathematics and the Department of Civil and Environmental Engineering (DICA) at Politecnico di Milano.

SPEED is designed to handle the simulation of large-scale seismic wave propagation problems including the coupled effect of the seismic fault rupture, the propagation path through Earth layers, localized geological irregularities, such as alluvial basins and topographic irregularities, and soil-structure interaction problems. The reader is referred to Mazzieri et al. (2013) and to the SPEED website, <http://speed.mox.polimi.it/>, for an exhaustive explanation of the mathematical framework of the method, the code features and its main applications. Based on a discontinuous version of the classical spectral element method (DGSEM), proposed by Antonietti et al. (2012), SPEED is naturally oriented to solve multi-scale numerical problems, using non-conforming meshes (h -adaptivity) and different polynomial approximation degrees (N -adaptivity) in the numerical model. This makes mesh design more flexible (since grid elements do not have to match across interfaces) and permits to select the best-fitted discretization parameters in each sub-region, depending on the dynamic properties of the media and/or geometric constraints, while controlling the overall accuracy of the approximation.

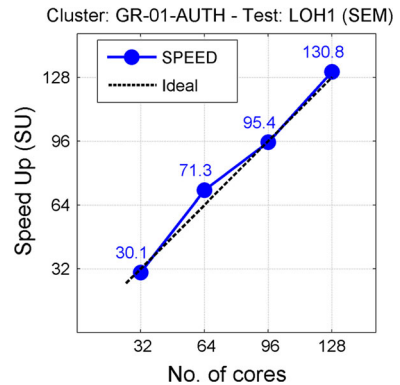
The present version of the SPEED includes the following features: (i) different seismic excitation modes, including kinematic finite-fault ruptures models or plane wave excitation; (ii) both linear and non-linear visco-elastic soil materials; (iii) different soil attenuation models with frequency proportional (Stupazzini et al. 2009) or frequency constant quality factor (Moczo et al. 2014); (iv) paraxial absorbing boundary conditions (Stacey 1988); (v) time integration by either the second order accurate explicit leap-frog scheme or the fourth order accurate explicit Runge–Kutta scheme.

Besides being verified over different international benchmarks, such as the case of Grenoble (Chaljub et al. 2010), recently, the code has been applied to the simulation of real earthquakes, such as the April 6th 2009 L'Aquila (Smerzini and Villani 2012), the February 22nd 2011 Christchurch seismic sequence (Guidotti et al. 2011) and the May 29th 2012 Po Plain earthquake (Paolucci et al. 2015), as well as for the analysis of soil-structure interaction effects related to the dynamic response of large infrastructures or city clusters (Mazzieri et al. 2013).

As a part of this research activity, SPEED has been compiled on the parallel computational resources provided by the Aristotle University of Thessaloniki (AUTH) Scientific Computing Center (<http://www.grid.auth.gr/en/>). The analysis of the performance of the code is illustrated herein; this is crucial because the applicability of the computational approach is conditioned on the possibility of tackling complex 3D numerical simulations with many degrees of freedom (or the order of tens of million) at a reasonable computational time.

As an illustrative example of the scalability of the code, Fig. 3 shows the speed-up SU (i.e., ratio of the computational time for a sequential simulation with a single core over that for a parallel simulation with a given number of cores) as a function of the number of cores, as computed on the AUTH institutional cluster GR-01-AUTH using the benchmark known in the literature as Layer Over a Halfspace test (referred to as LOH1, see Day and Bradley 2001). The reader is referred to Mazzieri et al. (2013) for further details on the

Fig. 3 Speed-up (SU) of the code SPEED on the AUTH cluster (GR-01-AUTH)



computational model for the LOH1 test. In this case, the speed-up has been calculated taking as reference the simulation with 24 cores. The performance of SPEED is excellent, being very close to the ideal situation (super-linear features are due to cache effects), as the code was optimized for Bluegene/Q architectures, like the FERMI cluster (Tier-0 machine) at CINECA, Italy (<http://www.cineca.it/>).

4 3D modeling of the Thessaloniki urban area

Based on the available data regarding both the characterization of the seismic sources and geological, geotechnical and geophysical aspects, a large-scale 3D numerical model was defined to predict earthquake ground motions in the Thessaloniki urban area.

Referring to Fig. 4, the spectral element model includes the following features, as key ingredients:

- ground topography as retrieved from 90 m SRTM Digital Elevation Model (<http://srtm.csi.cgiar.org/>);
- four seismogenic fault sources posing a hazard to the city of Thessaloniki (see Fig. 2), specifically, Gerakarou (i.e., the fault responsible of the 1978 Volvi earthquake), Langadhas, Angelochori and Souroti (the latter two being part of the Anthemountas fault system), as retrieved from the GreDaSS database together with literature works (Roumelioti et al. 2007);
- horizontally layered crustal model for deep rock materials (from Ameri et al. 2008), see Fig. 4;
- 3D soil model of the Thessaloniki bay area, based on the works by Anastasiadis et al. (2001) and Apostolidis et al. (2004); this will be addressed in greater detail in the following.

The mesh extends over a volume of about $82 \times 64 \times 31 \text{ km}^3$ and is discretized using an unstructured hexahedral conforming mesh with characteristic element size ranging from a minimum of $\sim 150 \text{ m}$ at ground surface inside the basin to 2000 m at the bottom of the model. The model consists of 753,211 spectral elements, resulting in approximately 60 million of total degrees of freedom, with a third order polynomial approximation degree. Considering a rule of thumb of 5 grid points per minimum wavelength for non-dispersive

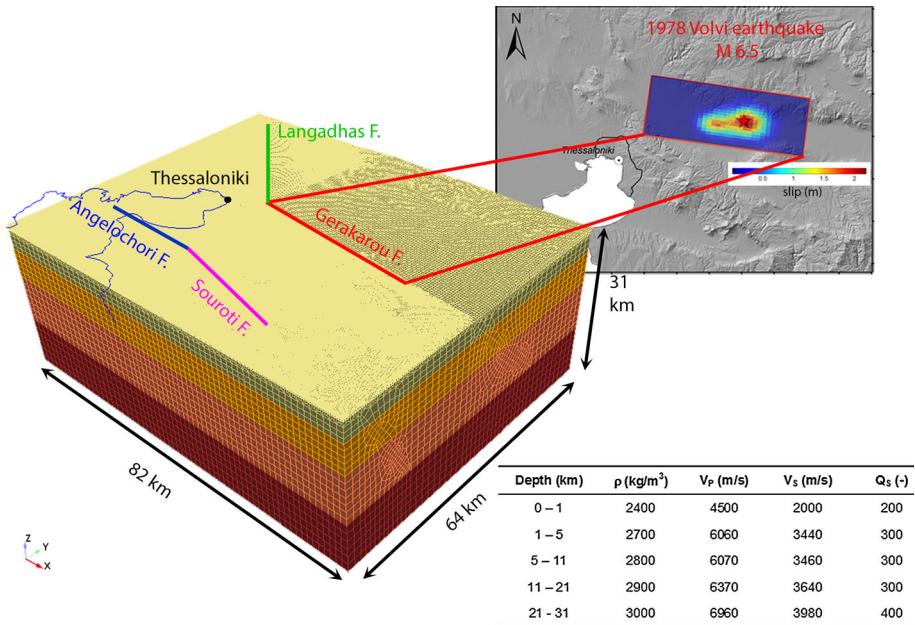


Fig. 4 3D spectral element mesh for the broader Thessaloniki area. The crustal model (from Ameri et al. 2008), the faults included in the model and the adopted slip distribution for the 1978 Volvi earthquake are also shown

wave propagation in heterogeneous media by the SE approach, this model can propagate frequencies up to about 1.5 Hz.

It is worth highlighting that the mesh incorporates the geometry of four different faults (Gerakarou, Langadhas, Angelochori and Souroti), as sketched in Fig. 4. Therefore, this model can be easily used to simulate fault rupture scenarios involving any of these seismic sources and to estimate the resulting ground motion in the broader Thessaloniki area.

To model the 3D subsurface structure, a reasonable balance had to be made between the thorough geophysical/geotechnical data available for the city and the need to simplify the mesh to avoid an excessive computational time and a level of detail that would not be captured within the frequency range propagated by such a large-scale model. In this perspective, the following assumptions were made:

- the 3D geometry of the geologic bedrock basement published by Apostolidis et al. (2004) (formation E in quoted paper) was included in the numerical model, as illustrated by the color map in Fig. 5 (left panel); a maximum depth of almost 800 m is reached in the southern promontory of the urban area (Kalamaria);
- two generic homogeneous soil profiles with linear visco-elastic behavior were defined for the alluvial deposits overlying the bedrock for sites belonging to Eurocode 8 - EC8 (CEN 2004) ground category B (average shear wave velocity in the top 30 m, $V_{S30} = 360\text{--}800$ m/s) and C ($V_{S30} = 180\text{--}360$ m/s), as mapped in Fig. 5 (right panel, after Pitilakis et al. 2015):

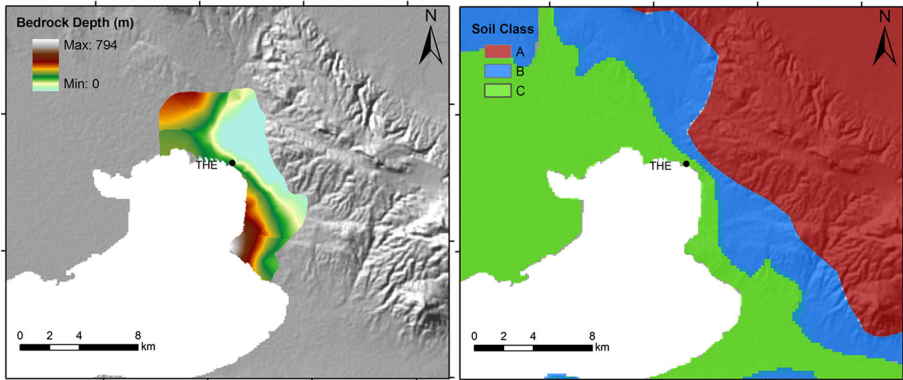


Fig. 5 *Left* 3D map showing the depth of geologic bedrock (after Apostolidis et al. 2004) within the city of Thessaloniki; the *color shades* denote the variations of bedrock depth in meters. *Right* simplified soil classification according to EC8 (based on Pitilakis et al. 2015)

for S (shear) and P (primary) wave velocity : $V_{S/P}(z)$

$$= V_{S/P,l} + (V_{S/P,m} - V_{S/P,l}) \cdot \left(\frac{z}{h}\right)^{0.70} \quad (1a)$$

for soil density : $\rho(z) = \rho_l + \frac{(\rho_m - \rho_l)}{h} \cdot z$ (1b)

for S-wave quality factor :

$$\begin{cases} Q_S(z) = 20 & \text{for } z \leq 50 \text{ m} \\ Q_S(z) = 50 & \text{for } 50 < z \leq 200 \text{ m} \\ Q_S(z) = 100 & \text{for } 200 < z \leq 500 \text{ m} \\ Q_S(z) = 150 & \text{for } 500 < z \leq 1000 \text{ m} \end{cases} \quad (1c)$$

with, z : depth from ground surface (in meters); $h = 1000$ m: maximum depth of profile up to geologic bedrock; $V_{S,l} = 500$ m/s (or 300 m/s) and $V_{P,l} = 2000$ m/s (or 1800 m/s): minimum S and P wave velocity for soil category B (or soil category C); $V_{S,m} = 2000$ m/s and $V_{P,m} = 4500$ m/s: maximum P and S wave velocity, corresponding to the velocity of outcrop rock formations (gneiss); $\rho_l = 2000$ kg/m³ and $\rho_m = 2400$ kg/m³: minimum and maximum soil density; Q_S : S wave quality factor at the reference frequency of 0.67 Hz (a frequency proportional quality factor is assumed).

The functional form for the V_S gradient was defined according to the recent findings achieved in the framework of NERA project (www.nera-eu-org), based on empirical data from SHARE-AUTH database (Pitilakis et al. 2014). The V_S profile was, then, calibrated from the available 1D profiles, as illustrated in Fig. 6. For V_P , the same gradient as for V_S was assumed; for soil density, a linear gradient was adopted, while for Q_S a step-like function was preferred. The latter was defined, on one side, by considering the average values as provided by Anastasiadis et al. (2001) for the main sediment formations present in the city and, on the other side, by constraining its behavior with depth on the basis of the relationships typically adopted in the literature, according to which Q_S can be reasonably estimated as $V_S/10$ (see e.g. Maufroy et al. 2015; Paolucci et al. 2015).

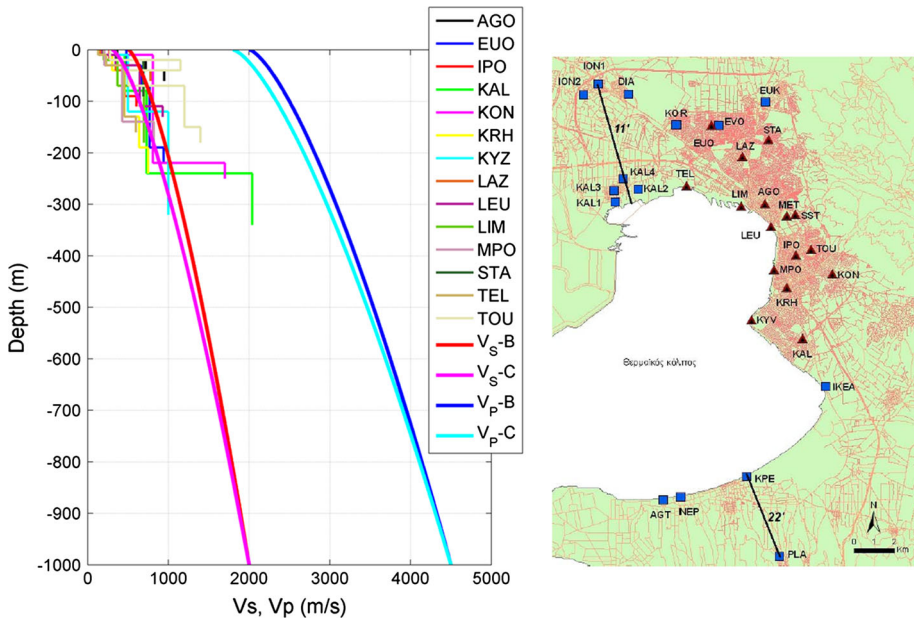


Fig. 6 Left average V_s/V_p profiles adopted for the 3D model, based on the available 1D data. Right location of the considered 1D profiles (triangles)

Note that the Apostolidis et al. (2004) model covers a small area compared to the whole 3D SPEED model. As the basin is not closed but is open to NW (Axios basin), SW (Thermaikos gulf) and SE (Anthemountas basin), it was necessary to extend the 3D soil model along these directions in an approximate way, considering the dominant surface geomorphological and geological features in the area.

5 Numerical simulation of the 1978 Volvi earthquake

As a case study, the M_w 6.5 June 20th 1978 Volvi earthquake was simulated by SPEED. The earthquake was a double event occurring at a distance of about 25 km northeast of the city on a nearly WNW-trending, NNE-dipping normal fault (Soufleris and Stewart 1981) along the SW margin of the Mygdonian graben. Note that validation purposes are beyond the scope of this work, because for this historical earthquake a limited amount of data is available. In particular, the earthquake was recorded by only one analog accelerometric station (THE-City Hotel) located at the basement of an 8 story RC building at the shoreline of the city.

To simulate the Volvi earthquake, in addition to the 3D soil features illustrated in previous section, a kinematic source model rupturing the Gerakarou fault was considered. Reference was made to the recent work by Roumelioti et al. (2007), who investigated the rupture process of the 1978 earthquake from the analysis of teleseismic waveforms, recorded in the distance range 21° to 37° , and near-fault levelling data. To the authors' knowledge, this work is the only one available in the literature providing the slip distribution; other papers are limited to the determination of fault plane solutions (e.g. Papazachos et al. 1979; Stiros and Drakos 2000). Based on some preliminary comparisons

between synthetics and observations, the following modifications were made with respect to the model published by Roumelioti et al. (2007), referred to as RO07 hereafter: (i) the top depth of rupture (Z_{top}) was assumed at 1 km to avoid super-shear effects (V_S in the top layer of crustal model is, in fact, 2 km/s); (ii) for the slip distribution, a k^{-2} slip model according to Herrero and Bernard (1994), referred to as “ k^{-2} model”, with location and size of the asperities resembling the main slip patch of the original model, was generated. The final kinematic source parameters are listed in Table 1 while the slip distribution is plotted in Fig. 4.

To clarify the impact of different assumptions regarding the source model, the results of these preliminary analyses are shown in Fig. 7 in terms of recorded vs simulated three-component (horizontal: EW, NS; vertical: UP) velocity waveforms (top panel) and corresponding Fourier amplitude spectra (FAS, bottom panel) at the accelerometric station THE-City Hotel. The analyses were performed through the Hisada code (Hisada and Bielak 2003), under the hypothesis of a 3D kinematic source model and a horizontally layered soil structure, assumed equal to the crustal model reported in Fig. 4. Black lines denote the strong motion observations (downloaded from ITSAK database: <http://www.itsak.gr/>), while colored lines indicate the Hisada simulations. Both synthetics and observations are filtered between 0.25 and 1.5 Hz. Specifically, the following parametric simulations were considered: (i) original source model by RO07, characterized by a focal mechanism (strike/dip/rake) of $278^\circ/46^\circ/-70^\circ$; (ii) same as in (i) but removing the superficial asperity from the slip distribution and rescaling the slip to preserve the total scalar seismic moment; (iii) proposed k^{-2} model, with geometry and focal mechanism equal to RO07; (iv) same as in (iii) but assuming the focal mechanism proposed by Papazachos et al. (1979), namely, $304^\circ/80^\circ/50^\circ$. The assumed slip distributions are illustrated on right hand side of Fig. 7. For comparison purposes, the same temporal axis is kept for all simulated time histories.

It is found that the original slip distribution by RO07, characterized by a significant slip asperity at ground surface (as inferred from leveling data), in conjunction with the assumed crustal model, induces unrealistic ground motion amplitudes and duration towards the city of Thessaloniki, especially on the EW and UP components, owing to excessive amplification effects around the resonance frequency of the first layer of the crustal model, i.e., at around 0.5 and 1 Hz for S and P waves, respectively. Such strong reverberations were found to vanish by adopting a different crustal model (e.g. by excluding the first 1000 m thick layer from the original crustal model). In spite of this shortcoming, the NS component is well predicted and frequencies above 1 Hz approximately are reproduced with a higher accuracy than the other models. Predictions change dramatically by removing the superficial asperity from the RO07 slip model: this points out the impact of up-dip asperities together with the assumed focal mechanism on seismic motion towards the city of Thessaloniki. On the other hand, the k^{-2} model provides satisfactory results in terms of

Table 1 Kinematic source parameters for the simulation of the 1978 Volvi earthquake. L = length, W = width, Ztop = top depth of rupture. Geographic coordinates are in WGS84

| Hypocenter (°N, °E) | Depth (km) | L × W (km ²) | Z _{top} (km) | Strike (°) | Dip (°) | Rake (°) | Rupture Vel (km/s) | Rise Time (s) |
|---------------------|------------|--------------------------|-----------------------|------------|---------|----------|--------------------|---------------|
| (40.705, 23.266) | 7.5 | 35 × 19 | 1 | 278 | 46 | −70 | 2.6 | 0.6 |

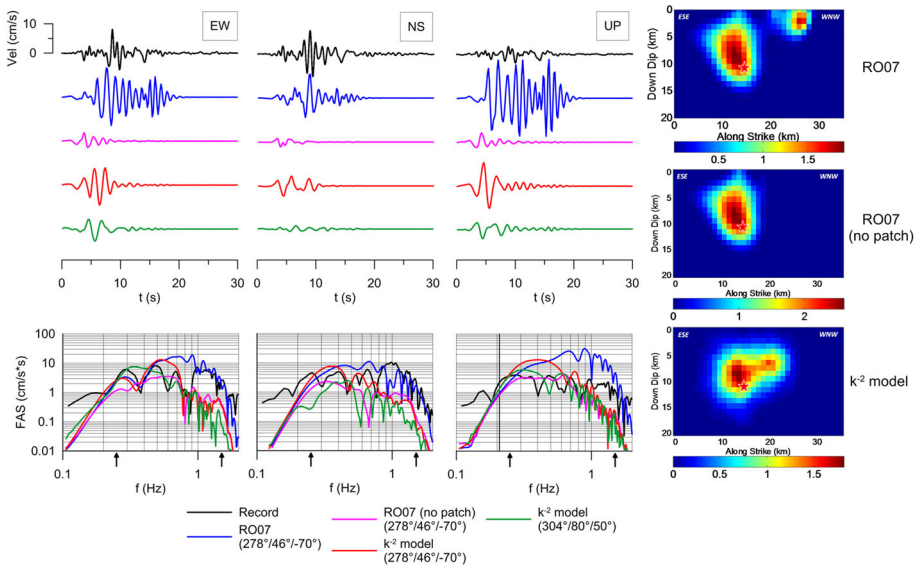


Fig. 7 Preliminary analyses with Hisada code: comparison between synthetics and observations at THE station in terms of three-component (EW, *left*; NS, *center*; UP, *right*) velocity time histories (*top panel*) and corresponding Fourier Amplitude Spectra (FAS, *bottom panel*) in the frequency range 0.25–1.5 Hz (as denoted by the superimposed arrows). The slip distribution of the considered source models is also depicted on the *right hand side*

ground motion amplitude and frequency content especially in the range 0–1 Hz, although it tends to underestimate observations for frequencies larger than 1 Hz. The assumption of the k^{-2} model but with a different focal mechanism (e.g. $304^{\circ}/80^{\circ}/50^{\circ}$) has a strong impact on results and leads to ground motion predictions which are generally significantly lower in amplitude (see in particular the UP component). Regarding the vertical component, it turns out that the model overprediction is influenced both by the slip distribution and the focal mechanism, being mainly related to the presence of up-dip asperities located along the direction of slip.

It is worth underlining that the scope of these analyses was not to calibrate an “ad hoc” finite-fault model maximizing the fit with observations, rather to evaluate the impact of different hypotheses regarding the source models, in perspective of the interpretation of the results which will be shown in the following sections.

5.1 Comparison between synthetics and observations

Based on the preliminary analyses with Hisada code, simulations were carried out by SPEED considering the fault model of Table 1 with the k^{-2} slip model and including the 3D soil structure beneath the city of Thessaloniki. As anticipated previously, given the scarcity of strong-motion observations for the Volvi event, the scope of the comparison shown herein is not to reproduce exactly the recorded waveforms, rather to check the capability of the numerical simulations to predict the general features of earthquake ground motion with a satisfactory level of accuracy.

Figure 8 shows the comparison between 3D synthetics and ground motion observations at THE station in terms of three-component velocity waveforms (*top panel*) and Fourier

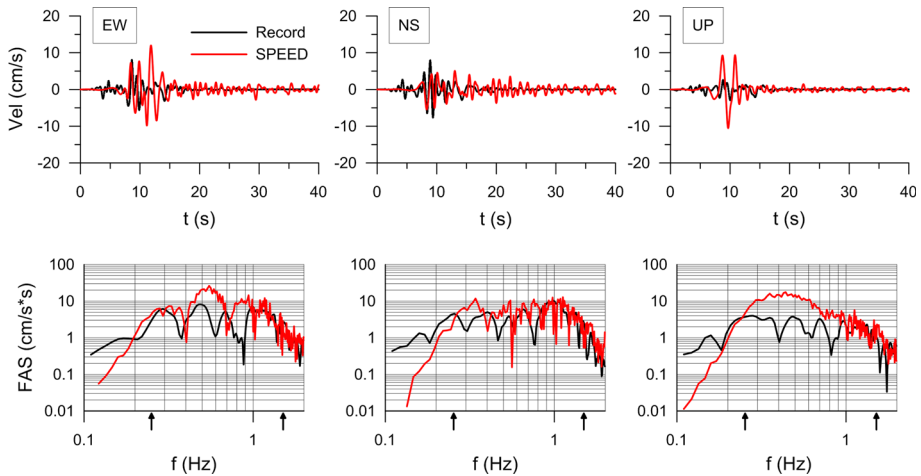


Fig. 8 SPEED results: comparison between synthetics and observations at THE station in terms of three component (EW, *left*; NS, *center*; UP, *right*) velocity time histories (*top panel*) and corresponding Fourier Amplitude Spectra (FAS, *bottom panel*). Data are band-passed filtered between 0.25 and 1.5 Hz, as denoted by the superimposed *arrows*

amplitude spectra (FAS, bottom panel) in the range of frequency 0.25–1.5 Hz. The former is the minimum usable frequency of the analog record while the latter is the frequency limit of the numerical simulation. Note that synthetics refer to a linear visco-elastic analysis. A satisfactory agreement is found for the horizontal components in terms of peak values and spectral content, especially for the NS component. Referring to the EW component, the later large amplitude (associated to surface waves propagation) is missing in the record and frequency components between about 0.4 and 1 Hz are overestimated by the numerical model, most likely due to assumptions regarding the subsoil structure and soil attenuation. With regard to the latter point, it should be remarked that the high-frequency content of synthetics tends to be higher than observations, suggesting that the adopted attenuation model is probably lower than the real one. Previous studies (see e.g. Anastasiadis et al. 2001; Raptakis and Makra 2010) indicate, in fact, that a peculiarity of the red silty clay formation, extended beneath the city, is the rather low Q_s , attaining minimum values of about 6–15 in the superficial soil layers, lower than the ones adopted in the 3D simulation. In spite of this shortcoming, the adoption of a non-linear soil model, calibrated on the available laboratory tests, is expected to improve the results, allowing for a better characterization of soil damping and its behavior with shear strain. These topics will be addressed in Sect. 6.2.

The vertical component is overestimated by the simulation, due to the assumptions regarding the up-dip slip asperities together with the focal mechanism, as confirmed by independent analyses performed through the Hisada code (see previous section).

5.2 Ground shaking maps

Interesting outputs of 3D numerical simulations are ground shaking maps at a broad scale in terms of different ground motion intensity measures, such as Peak Ground Velocity (PGV), Peak Ground Displacement (PGD) or response spectral acceleration (SA). In Fig. 9 the spatial distribution of both PGV (left) and SA at vibration period $T = 2$ s (right),

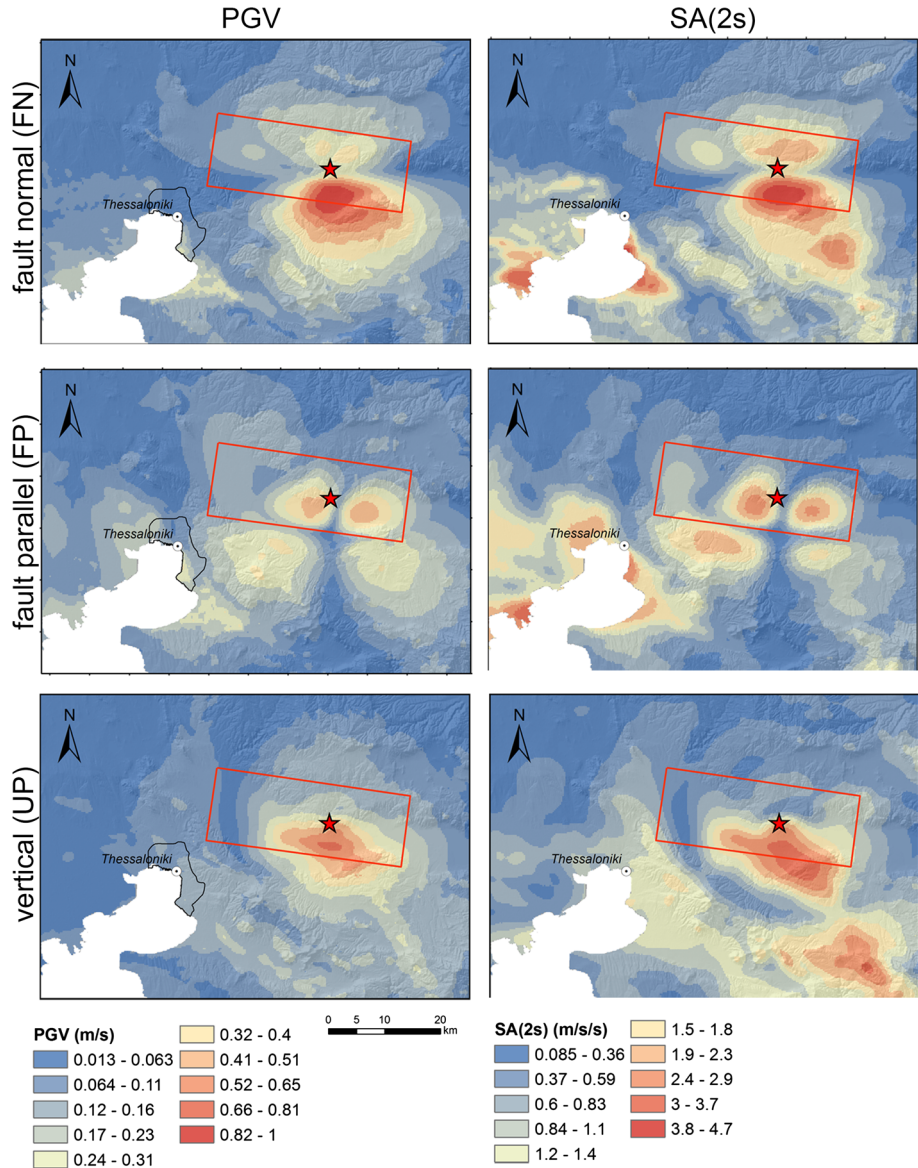


Fig. 9 Map of Peak Ground Velocity (PGV, left) and response spectral acceleration at 2 s (SA(2 s), right) for the Fault Normal (FN, top), Fault Parallel (FP, center) and vertical (UP, bottom) components

filtered in the range 0.05–1.5 Hz, is shown for the three components of ground motion: normal to the fault strike (Fault Normal: FN, top), parallel to the fault strike (Fault Parallel: FP, center) and vertical (UP, bottom). It is found that maximum PGV values of about 1 m/s are found on the hanging wall of the fault on the FN component, while the FP ground motions tend to be significant lower in the near field. Vertical motion can be larger than the horizontal FP motion in the near-source region, in agreement with the evidence of larger vertical to horizontal ratios in the proximity of the source (see e.g. Ambraseys and Douglas

2003). The spatial pattern of SA(2 s) emphasizes the role of the Thessaloniki basin on ground motion amplification.

It turns out that maximum ground motion amplitudes are found in the region, south-east of the epicenter owing to up-dip source directivity effects, with significant values of the FN/FP ratio up to one order of magnitude in the near field on the hangingwall of the fault, while, at larger distances, the proportion of FP motion with respect to the FN component increases in conjunction with the more relevant amplification of ground motion due to the presence of soft sedimentary deposits.

As a qualitative comparison of the accuracy of numerical simulations in predicting the spatial variability of ground motion at territorial scale, Fig. 10 illustrates the comparison between the map of the horizontal geometric mean of PGV (PGV_{gmh}) provided by SPEED simulations with the regional distribution of the Mercani-Cancani-Sieberg (MCS) intensities as inferred from post-earthquake surveys. MCS data were taken from Papazachos et al. (1997). Note that this comparison can be only qualitative owing to different reasons, such as: (i) computed PGV values are generally representative of a range of periods (0.5–1.0 s approximately) which does not necessarily coincide with the fundamental period of vibration of the constructions that were damaged; (ii) the 3D model does not account for the presence of other localized basins, such as the Volvi basin close to the earthquake epicenter, which may have affected the local seismic response.

With regard to the urban area of Thessaloniki, PGV_{gmh} ranges from 4 to 30 cm/s: values of about 10 cm/s are found at the port area, while maximum PGV_{gmh} values of about 30 cm/s are found in the southern promontory (Kalamaria area).

5.3 Comparison with Ground Motion Prediction Equations

The aim of this section is to compare the simulated ground motions with different Ground Motion Prediction Equations (GMPEs) to verify that modeling results are, on average, in line with empirical estimates, at least in the range of distances that is well constrained from

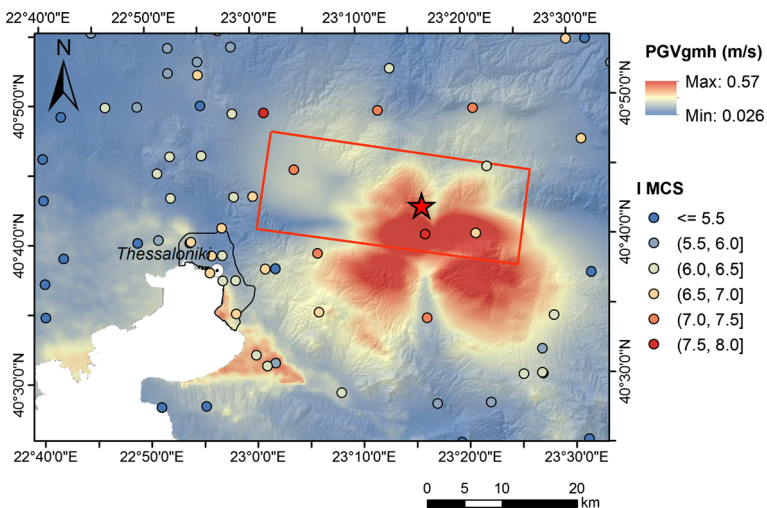


Fig. 10 Map of PGV_{gmh} (geometric mean of horizontal components) from the 3D numerical simulation, compared with the regional distribution of MCS intensity during the 1978 Volvi earthquake (from Papazachos et al. 1997)

recorded data (i.e. 20–40 km from the seismic source) and in absence of complex site effects. The comparison will be presented for two GMPEs and in terms of different ground motion parameters, namely, PGV and response spectral displacement (SD) at 1 s.

Figure 11 illustrates the comparison of the numerical results by SPEED with the GMPE by Skarlatoudis et al. (2003, 2007), referred to in the following as SK07, in terms of PGVgmh (a), and by Cauzzi et al. (2015), referred to as CEA15, in terms of SDgmh at 1 s (b), for both rock (left panel) and stiff/soft soil (right panel) conditions. Note that SK07 was developed specifically for shallow earthquakes in the broader Aegean area, while CEA15 is based on a worldwide dataset of digital acceleration records. Both GMPEs were computed for a normal focal mechanism with $M_w = 6.5$. Referring to SK07, an average focal depth $h_0 = 7$ km (as suggested by the authors) is assumed and site effects are quantified in a simplified way, by using two generic soil classes, “rock” and “basin”. For CEA15, the functional form modeling site effects in terms of dummy variables for the EC8 ground categories is adopted. Note that the two empirical models are defined for different distance metrics: epicentral distance R_{EPI} for SK07 and rupture distance R_{RUP} (minimum distance to the ruptured fault) for CEA15. Peak values from synthetics are computed considering a regular grid of points at ground surface covering the whole numerical model.

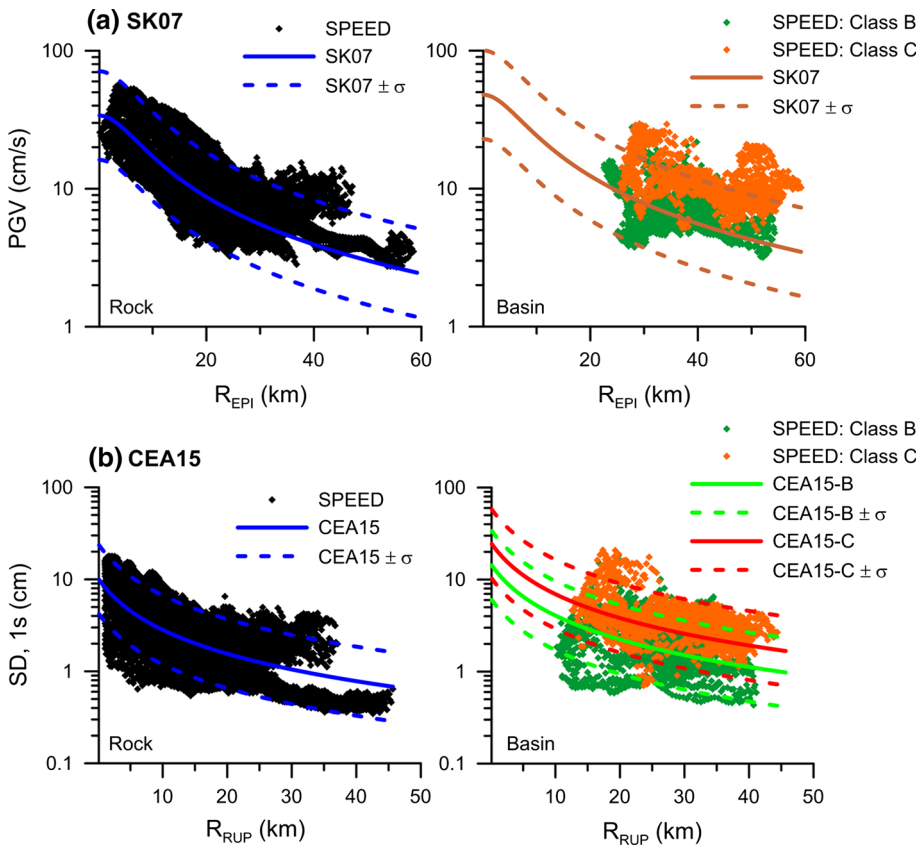


Fig. 11 Comparison of synthetics with the GMPEs by **a** Skarlatoudis et al. (2003, 2007), SK07 (*top*) and **b** Cauzzi et al. (2015), CEA15 (*bottom*), in terms of PGVgmh and SDgmh (1 s), respectively, for both rock (*left*) and basin (*right*) sites. R_{EPI} and R_{RUP} denote the epicentral and rupture distance, respectively

A good comparison is found between simulations and empirical estimates, especially at rock sites, being the numerical predictions mostly between the $\pm\sigma$ curves of both GMPEs. Some discrepancies found for soft sites (EC8 class C sites with $V_S = 300$ m/s), located in the Anthemountas and Axios-Vardar basin, especially when using SK07, most likely due to the inadequacy of the GMPE to account for complex localized site effects.

6 Evaluation of 3D site effects

This section aims at assessing 3D site effects within the Thessaloniki urban area making use of the numerical results by SPEED for the Volvi earthquake, focusing on the comparison between synthetic and experimental amplification functions at selected sites in the city (Sect. 6.1) as well as the effect of non-linear visco-elastic soil behavior (Sect. 6.2) and the spatial variability of site amplification factors (Sect. 6.3).

6.1 Comparison with experimental amplification functions

To verify the capability of the 3D model to predict site response effects within the Thessaloniki urban area, the experimental data available from a previous study, namely Lachet et al. (1996), were exploited. In this work the authors analyzed the dataset obtained from a temporary network of eleven three-component seismological stations that were in operation in the city of Thessaloniki between November 25th 1993 and February 19th 1994 to record earthquakes and ambient noise over various geological formations. The location of these stations is illustrated in Fig. 12.

To evaluate site response at the available stations the Standard Spectral Ratio (SSR) technique has been applied (Borcherdt 1970). This provides information on the ground motion amplification due to local geological conditions in the different parts of the city. Station OBS, which is located on outcrop basement, was used as a reference site, following the indications provided by Lachet et al. (1996). With reference to the numerical (SPEED) dataset, synthetic SSRs were computed for both EW and NS components as ratio of the smoothed (unfiltered) FAS of the horizontal motion at the target station on soil over the one at the reference station (OBS); then, the geometric mean of horizontal SSRs is calculated. A Konno-Omachi smoothing was applied to synthetics with bandwidth parameter $b = 40$.

The synthetic SSRs are compared in Fig. 12 with the experimental SSRs as published by Lachet et al. (1996) for the geometric mean of horizontal components. It should be remarked that experimental SSRs were computed considering a set of 40 small local earthquakes, with epicentral distances ranging from 1 to 11 km and magnitudes varying between 1.4 and 4.2, while synthetic curves are derived only for a single strong earthquake at larger distance (around 25 km). For this reason a full comparison should not be expected. For a couple of stations, namely LEP and ROT, the horizontal geometric mean of the SSRs published by Raptakis et al. (2004a), starting from the same dataset, is also illustrated. Note that experimental SSRs are not available for all stations: namely, for stations AGO, POL and THE, only synthetic curves are illustrated because of the poor accuracy of the observed ones in the range of frequency of interest for the comparison.

Overall, a satisfactory agreement between experimental and synthetic SSR curves is found, especially at sites closer to the historical center of Thessaloniki, such as LEP (White Tower station), ROT, OTE and TYF. Significant differences are found in the southern region at station KAL, where simulations predict a clear fundamental resonance frequency

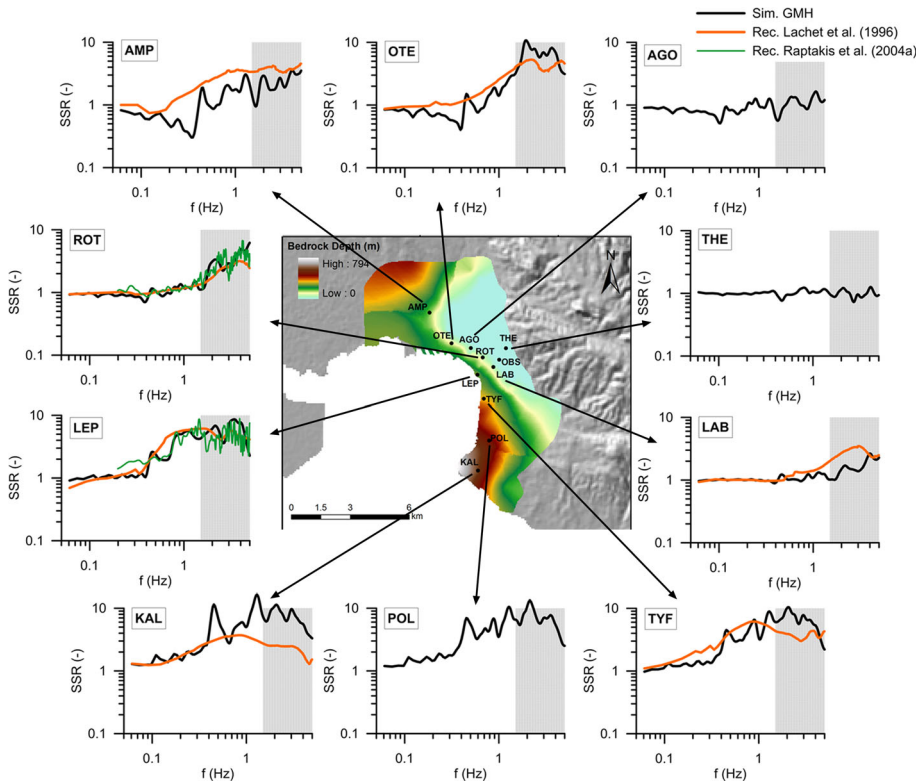


Fig. 12 Standard Spectral Ratios (SSRs) evaluated for a set of sites located in the Thessaloniki urban area, using OBS as a reference site on outcropping bedrock. The comparison between synthetic (*black line*) and experimental (*orange/green line*) curves derived by Lachet et al. (1996) and Raptakis et al. (2004a) is shown. The *shaded region* denotes the frequency range which is not captured by the 3D model

at around 0.5 Hz, which is not found in the recordings, and larger amplification in a broad frequency range above 1 Hz. Some discrepancies are obtained also at stations AMP and LAB, where the bedrock depth is particularly low (about 20 m and 35 m, from Lachet et al. 1996), most likely due the approximation introduced by the 3D discretization which is not sufficiently refined to catch such small scale variations. At these sites, numerical results tend to underestimate the experimental ratios. Finally, it should be noted that the largest differences are found at the farthest sites from the reference station OBS, where, thus, most likely SSRs are less accurate.

Taking advantage of a wider dataset of earthquake recordings provided by accelerographs installed by AUTH-LSMFGEE and ITSAK, a more thorough study focusing on the comparison between experimental and 3D/2D/1D amplification functions is foreseen in next future.

6.2 Effect of non-linear visco-elastic soil behavior

As a further improvement of the numerical model, the hypothesis of linearity has been removed by considering non-linear visco-elastic soil behavior. This is implemented in SPEED by introducing and generalizing to the 3D case the $G/G_{\max}-\gamma$ and $D-\gamma$ curves

adopted routinely in 1D equivalent-linear approaches (see e.g. Kramer 1996), where G (G_{\max}), D , and γ are the shear modulus (at small strains), the damping ratio and the shear strain, respectively. Note that, with respect to the classical equivalent-linear approach working in the frequency domain, in a time-advancing approach like SPEED, at each generic time of the simulation the values of G and D are updated using a suitable scalar measure of the ground strain tensor (Stupazzini et al. 2009).

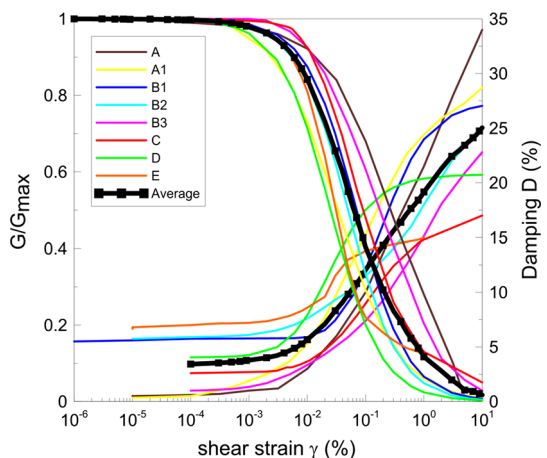
For the Thessaloniki case study, a single set of G/G_{\max} - γ and D - γ curves was adopted for the top 100 m of soil deposits. These curves have been calibrated by considering the average of the results of dynamic laboratory tests conducted on the main soil formations by Anastasiadis et al. (2001), as illustrated in Fig. 13.

To shed light on the effect of soil non-linearities, in Fig. 14 the horizontal (EW and NS) velocity time histories computed for both linear (LE: black line) and non-linear (NLE: red line) visco-elastic behavior are shown for a set of receivers along a representative cross-section HH', passing through the southern part of the city. It can be observed that the impact of non-linearity is rather limited and affects predominantly the coda of the signals, due to the moderate level of ground shaking and the relatively limited range of frequencies propagated by the model. Such effects can be better appreciated in Fig. 15, where the three-component velocity time histories and corresponding FAS are shown at two representative sites, namely, the strong motion station THE (top panel, a) and the receiver no. 16824 of cross-section HH' (bottom panel, b), for both LE and NLE models. At the recording station THE non-linear effects turn out to be very limited due to the low ground shaking attained in this part of the city. On the other hand, the non-linear effects become appreciable for station 16824, where larger ground motion amplitudes are found owing to site amplification effects, at frequencies larger than about 0.8 Hz. In general, the NL model helps improve the results by attenuating the high-frequency content of ground motion, which was found generally higher than observations from previous discussion.

6.3 Spatial variability of site amplification factors

To give an overview of the 3D site response effects obtained within the urban area of Thessaloniki, amplification factors were determined over a sufficiently dense grid of

Fig. 13 Experimental G/G_{\max} - γ and D - γ curves derived by Anastasiadis et al. (2001) for the calibration of the non-linear visco-elastic soil model. The average curve (black line) has been adopted for the top 100 m of soil deposits in the numerical model



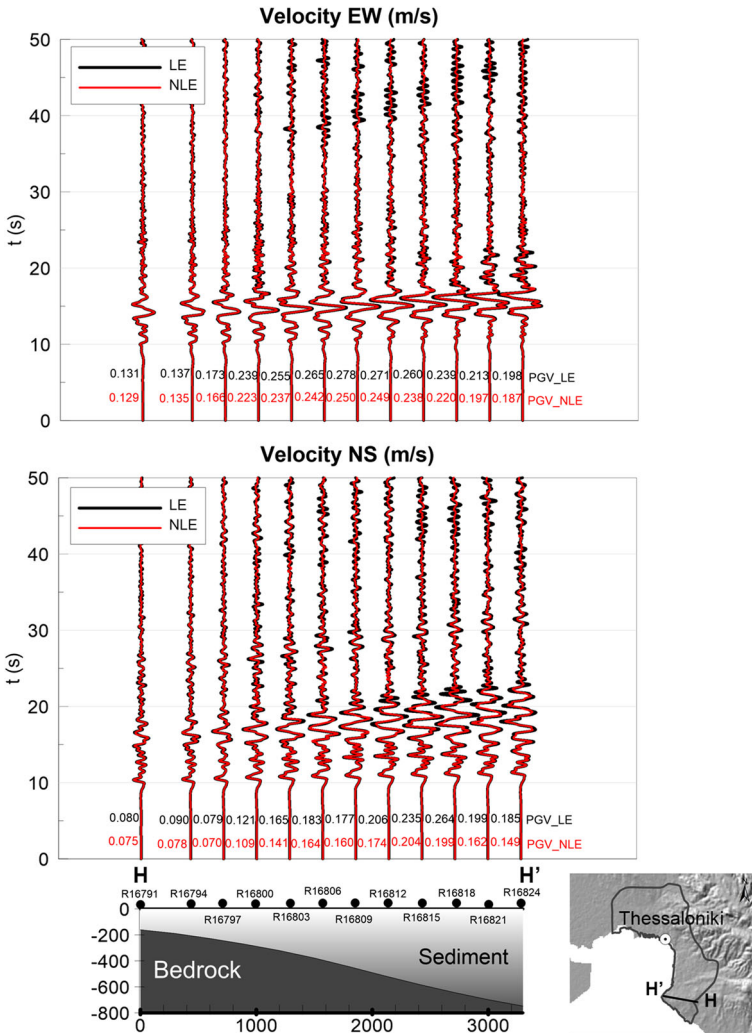


Fig. 14 Simulated EW (*top*) and NS (*bottom*) velocity waveforms computed by SPEED along a representative cross-section HH' (see location in the *right bottom map*) under the assumption of both linear (LE: *black line*) and non-linear (NLE: *red line*) visco-elastic soil behavior. PGV values (PGV_{LE} and PGV_{NLE}) are also superimposed on the plot at the beginning of each trace

receivers as ratio of a given ground motion parameter (e.g. PGV) on soil, as computed by SPEED considering the 3D subsurface structure with non-linear behavior (see Sect. 6.2), over the corresponding prediction for outcrop bedrock basement conditions. Therefore, for any site, the 3D amplification factor on a generic ground motion intensity measure IM is computed as $IM_{soil}^{3D}/IM_{rock_outcrop}^{1D}$, where IM_{soil}^{3D} refers to the simulation of the 3D wavefield radiated by the extended seismic source combined with the 3D subsurface structure while $IM_{rock_outcrop}^{1D}$ is estimated by considering the 3D wavefield propagating through the 1D layered crustal rock structure. Note that, given the modeling hypotheses regarding the crustal model, competent conditions refer to the geologic bedrock with $V_S = 2000$ m/s

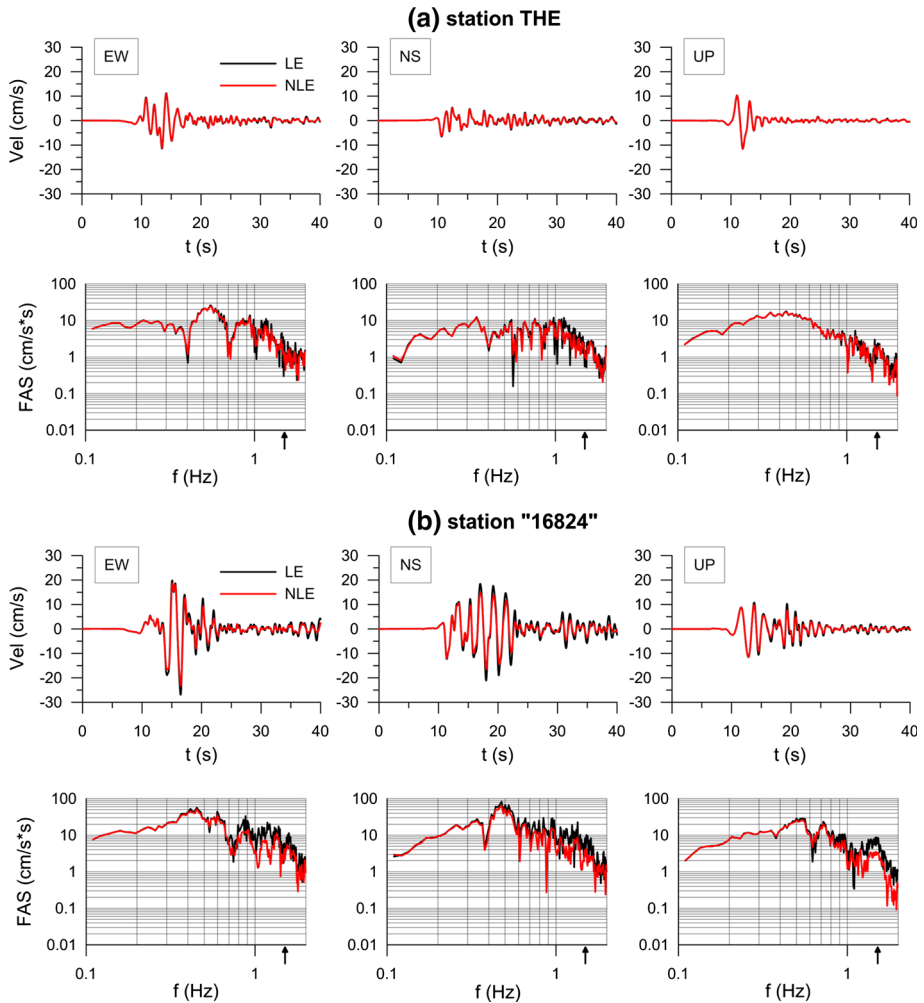


Fig. 15 Comparison between linear (LE: *black line*) and non-linear (NLE: *red line*) models at two representative receivers, **a** THE station (*top*) and **b** receiver no. 16824 (*bottom*), located along the HH' cross-section of Fig. 14, in terms of three-component velocity time histories (*top panels*) and corresponding FAS (*bottom panels*)

rather than the seismic bedrock ($V_s = 800$ m/s). Note that the synthetics were filtered in the range 0.05–1.5 Hz.

Figure 16 shows the spatial variability of the site amplification ratios computed for the following parameters in terms of geometric mean of horizontal component: PGV, PGD, SA(1 s) and SA(2.0 s). These maps point out clearly the strong connection between the soil amplification pattern and the 3D subsoil structure. Maximum amplification factors of 2.4 and 3.2 are found in the north-western sector of the city for PGV and PGD, respectively, while for SA higher values, up to 6.2 for 1 s and 4 for 2 s, are found in the southern region, where the depth of bedrock reaches its maximum values (see Fig. 5).

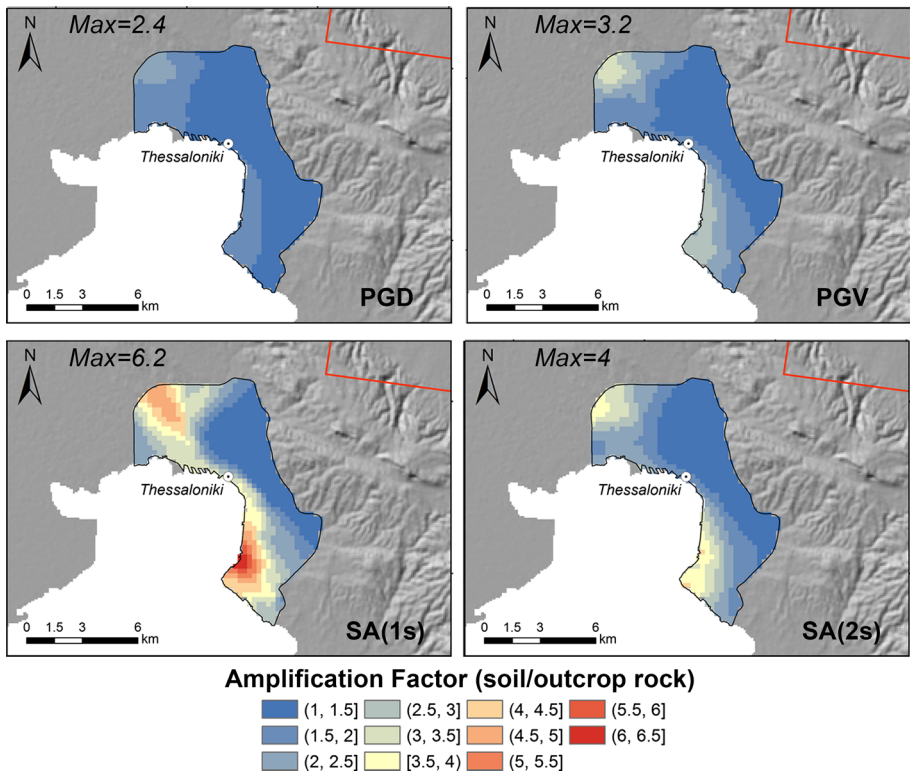


Fig. 16 Map of site amplification factors for PGD, PGV and SA(1 s) and SA(2 s), geometric mean of horizontal components, computed as ratios of predictions obtained with the 3D non-linear soil model and the ones with outcropping bedrock

7 Concluding remarks

In this paper 3D numerical modeling of earthquake ground motion in the Thessaloniki urban area has been addressed with particular reference to the simulation of the destructive M_w 6.5 June 20th 1978 earthquake, which affected seriously the city. Although the validation of the numerical model for this earthquake is beyond the scope of this work due to the limited availability of strong motion recordings, it was considered interesting to analyze the main features of spatial variability of earthquake ground motion during a major earthquake like the historical Volvi earthquake, with emphasis on the aspects related to local site response.

A large scale model by spectral elements (code: SPEED) was generated up to maximum frequencies of about 1.5 Hz, including a simplified description of the 3D subsoil structure of the urban area, as retrieved from previous geotechnical and geophysical studies, as well as the extended seismic sources posing a serious threat to the city of Thessaloniki.

Comparison between simulations and observations in terms of ground motion time histories at the only available strong-motion station (THE-City Hotel) as well as of spatial distribution of peak parameters, as compared to the distribution of macroseismic (MCS) intensity and to GMPES, has shown that reasonable estimates can be achieved in the frequency range of the numerical model. Ground shaking maps in terms of PGV and SA

are provided to shed light on the most significant wave propagation effects, such as near-fault and focal mechanism effects combined with complex site response.

Site response in the urban area of Thessaloniki has been studied through the SSR technique and, as a further validation of the simulations, comparison with a set of available recordings from local earthquakes of small magnitude has pointed out that the 3D model is capable of predicting the main local amplification features especially at sites closer to the Thessaloniki historical center. A non-linear soil model has been also investigated, showing the occurrence of limited effects due to the moderate ground motion intensity levels attained in the city for the considered rupture scenario. Finally, maps of site amplification factors on PGV, PGD and SA are provided and indicate that relevant amplification factors, up to about 6, can be found on response spectral ordinates at intermediate to long periods, i.e. ≥ 1 s, in the southern sector of the city, at least for the deterministic scenario under consideration.

Results of this study demonstrate the potentialities of 3D physics-based numerical modelling for deterministic-based seismic hazard assessment studies in high seismicity areas characterized by complex geological configurations, such as the Thessaloniki area. The model presented in this study may be used to generate physics-based ground shaking scenarios from future earthquakes affecting the city of Thessaloniki and resulting from hypothetical fault breaks involving the Gerakarou, Langadhas or Anthemountas seismogenic sources.

Physics-based numerical simulations of earthquake ground motion, including a full 3D model from the source to the site, are expected to become, in near future, the most promising tool to generate ground shaking scenarios from future realistic earthquakes, as an alternative to standard empirical approaches based on the use of GMPEs, especially for the following aims: (i) better constrained seismic hazard assessment in those magnitude and distance ranges which are poorly constrained by recorded data, i.e., typically in the near field and for large magnitude earthquakes ($M_w > 7.0\text{--}7.5$); (ii) for seismic hazard and risk assessment studies of large urban areas, where the systemic and inter-connected nature of utility systems, infrastructures and spatially extended facilities together with the heterogeneity of the vulnerable elements (sensitive to different intensity measures) make necessary to preserve the full spatial correlation of earthquake ground motion; (iii) for critical infrastructures, such as nuclear power plants or spatially extended infrastructures, for which a detailed simulation of the physics of the earthquake may have a great impact on site-specific hazard estimates (more accurate median values and reduction of epistemic uncertainty); (iv) deeper understanding of the variability of earthquake ground motion and of its spatial correlation features resulting from the complex combination of the fault rupture process and wave propagation effects (source directivity, non-linear behavior, 3D complex site effects). Conversely, the price to pay for such advantages is given by: (i) frequency limitation of the deterministic simulations, hardly larger than 2 Hz approximately; (ii) computational cost, implying, on one side, the use of parallel computer architectures to have, for each target simulation, reasonable computer times, and, on the other hand, limiting the range of possible scenarios to simulate in a Monte Carlo approach; (iii) the level of detail of the physical models for the geo-morphology of the region, which limits the application of such approaches only to a few areas worldwide.

Acknowledgments This study has been carried out in the framework of the STREST Project “Harmonised approach to stress tests for critical infrastructures against natural hazards”, EU FP7/2007-2013, Grant Agreement No. 603389. The contributions of different researchers of the Aristotle University of Thessaloniki, namely Dr. Zafeiria Roumelioti, for providing the kinematic slip distribution for the 1978 earthquake,

Dr. Maria Manakou and Dr. Sotiris Argyroudis, for making available the data regarding the 3D model, Dr. Evi Riga, for providing information about the soil classification, Prof. D. Raptakis, for providing the experimental SSRs and for his fruitful comments regarding the analyses presented in the paper, are greatly acknowledged. The authors are also indebted to the staff of the AUTH Scientific Computing Center (SCC), in particular to Alexandra Charalampidou and Paschalis Korosoglou, for allowing the extensive use of the AUTH cluster and for providing technical support. The authors extend their gratitude to Prof. R. Paolucci and another anonymous reviewer for fruitful comments and suggestions, which helped improve the quality of the paper.

References

- Ambraseys N, Douglas J (2003) Near-field horizontal and vertical earthquake ground motions. *Soil Dyn Earthq Eng* 23:1–18. doi:[10.1016/S0267-7261\(02\)00153-7](https://doi.org/10.1016/S0267-7261(02)00153-7)
- Ameri G, Pacor F, Cultrera G, Franceschina G (2008) Deterministic ground-motion scenarios for engineering applications: the case of Thessaloniki, Greece. *Bull Seismol Soc Am* 98(3):1289–1303. doi:[10.1785/0120070114](https://doi.org/10.1785/0120070114)
- Anastasiadis A, Raptakis D, Ptilakis K (2001) Thessaloniki's detailed microzoning: subsurface structure as basis for site response analysis. *Pure Appl Geophys* 158:2597–2633. doi:[10.1007/PL00001188](https://doi.org/10.1007/PL00001188)
- Antonietti PF, Mazzieri I, Quarteroni A, Rapetti F (2012) Non-conforming high order approximations of the elastodynamics equation. *Comput Methods Appl Mech Eng* 209–212:212–238. doi:[10.1016/j.cma.2011.11.004](https://doi.org/10.1016/j.cma.2011.11.004)
- Apostolidis P, Raptakis D, Roumelioti Z, Ptilakis K (2004) Determination of S-wave velocity structure using microtremors and SPAC method applied in Thessaloniki (Greece). *Soil Dyn Earthq Eng* 24:49–67. doi:[10.1016/j.soildyn.2003.09.001](https://doi.org/10.1016/j.soildyn.2003.09.001)
- Argyroudis S, Selva J, Kakderi K, Ptilakis K (2014) Application to the city of Thessaloniki. In: SYNER-G: systemic seismic vulnerability and risk assessment of complex urban, utility, lifeline systems and critical facilities, vol 31 of the series Geotechnical, Geological and Earthquake Engineering, Chapter 7, pp 199–240
- Bielak J, Ghattas O, Kim EJ (2005) Parallel octree-based finite element method for large-scale earthquake ground motion simulation. *Comput Model Eng Sci* 10:99–112. doi:[10.3970/cmesc.2005.010.099](https://doi.org/10.3970/cmesc.2005.010.099)
- Borcherdt RD (1970) Effects of local geology on ground motion near San Francisco Bay. *Bull Seismol Soc Am* 60:29–61
- Caputo R, Chatzipetros A, Pavlides S, Sboras S (2012) The Greek database of seismogenic sources (GreDaSS): state-of-the-art for northern Greece. *Ann Geophys Italy* 55(5):859–894. doi:[10.4401/ag-5168](https://doi.org/10.4401/ag-5168)
- Cauzzi C, Faccioli E, Vanini M, Bianchini A (2015) Updated predictive equations for broadband (0.01–10 s) horizontal response spectra and peak ground motions, based on a global dataset of digital acceleration records. *Bull Earthq Eng* 13:1587–1612. doi:[10.1007/s10518-014-9685-y](https://doi.org/10.1007/s10518-014-9685-y)
- CEN (2004) Eurocode 8: design provisions for earthquake resistance of structures, part 1.1: general rules, seismic actions and rules for buildings. European Committee for Standardization, Pren1998-1
- Chaljub E, Moczo P, Tsuno S, Bard PY, Kristek J, Käser M, Stupazzini M, Kristekova M (2010) Quantitative comparison of four numerical predictions of 3D ground motion in the Grenoble valley, France. *Bull Seismol Soc Am* 100(4):1427–1455. doi:[10.1785/0120090052](https://doi.org/10.1785/0120090052)
- Day SM, Bradley CR (2001) Memory-efficient simulation of anelastic wave propagation. *Bull Seismol Soc Am* 91(3):520–531. doi:[10.1193/1.2857545](https://doi.org/10.1193/1.2857545)
- Faccioli E, Maggio F, Paolucci R, Quarteroni A (1997) 2D and 3D elastic wave propagation by a pseudo-spectral domain decomposition method. *J Seismol* 1(3):237–251. doi:[10.1023/A:1009758820546](https://doi.org/10.1023/A:1009758820546)
- Graves RW (1996) Simulating seismic wave propagation in 3D elastic media using staggered-grid finite differences. *Bull Seismol Soc Am* 86(4):1091–1106
- Graves R, Jordan T, Callaghan S, Deelman E, Field E, Juve G, Kesselman C, Maechling P, Mehta G, Milner K, Okaya D, Small P, Vahi K (2011) CyberShake: a physics-based seismic hazard model for Southern California. *Pure Appl Geophys* 168(3–4):367–381. doi:[10.1007/s00024-010-0161-6](https://doi.org/10.1007/s00024-010-0161-6)
- Guidotti R, Stupazzini M, Smerzini C, Paolucci R, Ramieri P (2011) Numerical study on the role of basin geometry and kinematic seismic source in 3D ground motion simulation of the 22 February 2011 M_w 6.2 Christchurch earthquake. *Seismol Res Lett* 82(6):767–782
- Herrero A, Bernard P (1994) A kinematic self-similar rupture process for earthquakes. *Bull Seismol Soc Am* 84(4):1216–1228

- Hisada Y, Bielak J (2003) A theoretical method for computing near-fault ground motions in layered half-spaces considering static offset due to surface faulting, with a physical interpretation of fling step and rupture directivity. *Bull Seismol Soc Am* 93(3):1154–1168. doi:[10.1785/0120020165](https://doi.org/10.1785/0120020165)
- Komatitsch D, Vilotte JP (1998) The spectral-element method: an efficient tool to simulate the seismic response of 2D and 3D geological structures. *Bull Seismol Soc Am* 88(2):368–392
- Kramer SL (1996) *Geotechnical earthquake engineering*. Prentice Hall, Upper Saddle River
- Lachet C, Hatzfeld D, Bard PY, Theodulidis N, Papaioannou Ch, Savva A (1996) Site effects and microzonation in the city of Thessaloniki (Greece) comparison of different approaches. *Bull Seismol Soc Am* 86:1692–1703
- Maufroy E, Chaljub E, Hollender F, Kristek J, Moczo P, Klin P, Priolo E, Iwaki A, Iwata T, Etienne V, De Martin F, Theodoulidis N, Manakou M, Guyonnet-Benaize C, Ptilakis K, Bard P-Y (2015) Earthquake ground motion in the Mygdonian basin, Greece: the E2VP verification and validation of 3D numerical simulation up to 4 Hz. *Bull Seismol Soc Am* 105(3):1398–1418. doi:[10.1785/0120140228](https://doi.org/10.1785/0120140228)
- Mazzieri I, Stupazzini M, Guidotti R, Smerzini C (2013) SPEED: Spectral elements in elastodynamics with discontinuous Galerkin: a non-conforming approach for 3D multi-scale problems. *Int J Numer Methods Eng* 95(12):991–1010
- Moczo P, Kristek J, Galis M (2014) *The finite-difference modelling of earthquake motions: waves and ruptures*. Cambridge University Press, Cambridge
- Paolucci R, Mazzieri I, Smerzini C, Stupazzini M (2014) Physics-based earthquake ground shaking in large urban areas. In: Ansal A (ed) *Perspectives on European earthquake engineering and seismology, geotechnical, geological and earthquake engineering*, Chapter 10, vol 34. Springer, Berlin, pp 331–359. doi:[10.1007/978-3-319-07118-3_10](https://doi.org/10.1007/978-3-319-07118-3_10)
- Paolucci R, Mazzieri I, Smerzini C (2015) Anatomy of strong ground motion: near-source records and 3D physics-based numerical simulations of the Mw 6.0 May 29 2012 Po Plain earthquake, Italy. *Geophys J Int* 203:2001–2020. doi:[10.1093/gji/ggv405](https://doi.org/10.1093/gji/ggv405)
- Papazachos BC, Mountrakis D, Psilovikos A, Leventakis G (1979) Surface fault traces and fault plane solutions of May–June 1978 major shocks in the Thessaloniki area. *Tectonophysics* 53:171–183
- Papazachos BC, Papaioannou C, Papazachos CB, Savva AS (1997) *Atlas of isoseismal maps for strong shallow earthquakes in Greece and surrounding area (426BC–1995)*. Ziti Publications, Thessaloniki, p 192
- Papazachos BC, Comninakis PE, Karakaisis GF, Karakostas BG, Papaioannou CA, Papazachos CB, Scordilis EM (2000) *A catalogue of earthquakes in Greece and surrounding area for the period 550BC–1999*. Publ Geophys Laboratory University of Thessaloniki
- Papazachos BC, Comninakis PE, Scordilis EM, Karakaisis GF, Papazachos CB (2010) *A catalogue of earthquakes in the Mediterranean and surrounding area for the period 1901–2010*. Publ Geophys Laboratory University of Thessaloniki
- Paradisopoulou PM, Karakostas VG, Papadimitriou EE, Tranos MD, Papazachos CB, Karakaisis GF (2006) Microearthquake study of the broader Thessaloniki area (Northern Greece). *Ann Geophys Italy* 49(4/5):1081–1093. doi:[10.4401/ag-3112](https://doi.org/10.4401/ag-3112)
- Pitarka A (1999) 3D elastic finite-difference modeling of seismic motion using staggered grids with nonuniform spacing. *Bull Seismol Soc Am* 89(1):54–68
- Ptilakis K (2010) *Geotechnical earthquake engineering*, editions Ziti, pp 752. ISBN 978-960-456-226-8
- Ptilakis K, Riga E, Makra K, Gelagoti F, Ktenidou O-J, Anastasiadis A, Ptilakis D, Izquierdo Flores CA (2014) Deliverable D11.5 code cross-check, computed models and list of available results—AUTH contribution, network of European research infrastructures for earthquake risk assessment and mitigation (NERA), seventh framework programme. EC Project Number: 262330
- Ptilakis K, Riga E, Anastasiadis A (2015) New design spectra in Eurocode 8 and preliminary application to the seismic risk of Thessaloniki, Greece. In: Ansal A, Sakr M (eds) *Perspectives on earthquake geotechnical engineering*, series: geotechnical, geological and earthquake engineering, vol 37. Springer, Dordrecht, pp 45–91. doi:[10.1007/978-3-319-10786-8_3](https://doi.org/10.1007/978-3-319-10786-8_3)
- Porter K, Jones L, Cox D, Goltz J, Hudnut K, Milet D, Perry S, Ponti D, Reichle M, Rose AZ, Scawthorn CR, Seligson HA, Shoaf KI, Treiman J, Wein A (2011) The ShakeOut scenario: a hypothetical Mw7.8 earthquake on the Southern San Andreas Fault. *Earthq Spectra* 27:239–261. doi:[10.1193/1.3563624](https://doi.org/10.1193/1.3563624)
- Raptakis D, Makra K (2010) Shear wave velocity structure in western Thessaloniki (Greece) using mainly alternative SPAC method. *Soil Dyn Earthq Eng* 30(4):202–214. doi:[10.1016/j.soildyn.2009.10.006](https://doi.org/10.1016/j.soildyn.2009.10.006)
- Raptakis D, Makra K, Anastasiadis A, Ptilakis K (2004a) Complex site effects in Thessaloniki (Greece). Part I. Soil structure and comparison of observations with 1D analysis. *Bull Earthq Eng* 2:271–300. doi:[10.1007/s10518-004-3799-6](https://doi.org/10.1007/s10518-004-3799-6)

- Raptakis D, Makra K, Anastasiadis A, Pitolakis K (2004b) Complex site effects in Thessaloniki (Greece). Part II. 2D SH modeling and engineering insights. *Bull Earthq Eng* 2:301–327. doi:[10.1007/s10518-004-3803-1](https://doi.org/10.1007/s10518-004-3803-1)
- Roumelioti Z, Theodulidis N, Kiratzi A (2007) The 20 June 1978 Thessaloniki (Northern Greece) earthquake revisited: slip distribution and forward modelling of geodetic and seismological observations. In: 4th international conference on earthquake geotechnical engineering, June 25–28, Paper No. 1594
- Skarlatoudis AA, Papazachos CB, Margaritis BN, Theodulidis N, Papaioannou C, Kalogeras I, Scordilis EM, Karakostas V (2003) Empirical peak ground-motion predictive relations for shallow earthquake in Greece. *Bull Seismol Soc Am* 93(6):2591–2603. doi:[10.1785/0120030016](https://doi.org/10.1785/0120030016)
- Skarlatoudis AA, Papazachos CB, Margaritis BN, Theodulidis N, Papaioannou C, Kalogeras I, Scordilis EM, Karakostas V (2007) Erratum of “Empirical peak ground-motion predictive relations for shallow earthquake in Greece—B Seismol Soc Am, 93(6):2591–2603”. *Bull Seismol Soc Am* 97(6):2591–2603. doi:[10.1785/0120070176](https://doi.org/10.1785/0120070176)
- Skarlatoudis AA, Papazachos CB, Theodoulidis N, Kristek J, Moczo P (2010) Local site-effects for the city of Thessaloniki (N. Greece) using a 3-D finite-difference method: a case of complex dependence on source and model parameters. *Geophys J Int* 182:279–298. doi:[10.1111/j.1365-246X.2010.04606.x](https://doi.org/10.1111/j.1365-246X.2010.04606.x)
- Skarlatoudis AA, Papazachos CB, Theodoulidis N (2011) Spatial distribution of site effects and wave propagation properties in Thessaloniki (N. Greece) using a 3-D finite difference method. *Geophys J Int* 185:485–513. doi:[10.1111/j.1365-246X.2011.04954.x](https://doi.org/10.1111/j.1365-246X.2011.04954.x)
- Skarlatoudis AA, Papazachos CB, Theodoulidis N (2012) Site-response study of Thessaloniki (Northern Greece) for the 4 July 1978 M 5.1 aftershock of the June 1978 M 6.5 sequence using a 3D finite-difference approach. *Bull Seismol Soc Am* 102(2):722–737. doi:[10.1785/0120110136](https://doi.org/10.1785/0120110136)
- Smerzini C, Villani M (2012) Broadband numerical simulations in complex near field geological configurations: the case of the MW 6.3 2009 L'Aquila earthquake. *Bull Seismol Soc Am* 102(6):2436–2451. doi:[10.1785/0120120002](https://doi.org/10.1785/0120120002)
- Soufleris C, Stewart G (1981) A source study of the Thessaloniki (northern Greece) 1978 earthquake sequence. *Geophys J Int* 67:343–358
- Stacey R (1988) Improved transparent boundary formulations for the elastic-wave equation. *Bull Seismol Soc Am* 78(6):2089–2097
- Stiros SC, Drakos A (2000) Geodetic constrain on the fault pattern of the 1978 Thessaloniki (Northern Greece) earthquake (MS = 6.4). *Geophys J Int* 143:679–688. doi:[10.1046/j.1365-246X.2000.00249.x](https://doi.org/10.1046/j.1365-246X.2000.00249.x)
- Stupazzini M, Paolucci R, Igel H (2009) Near-fault earthquake ground-motion simulation in Grenoble Valley by high-performance spectral element code. *Bull Seismol Soc Am* 99(1):286–301. doi:[10.1785/0120080274](https://doi.org/10.1785/0120080274)
- Tranos MD, Papadimitriou EE, Kiliadis AA (2003) Thessaloniki-Gerakarou fault zone (TGFZ): the western extension of the 1978 Thessaloniki earthquake fault (Northern Greece) and seismic hazard assessment. *J Struct Geol* 25:109–2123. doi:[10.1016/S0191-8141\(03\)00071-3](https://doi.org/10.1016/S0191-8141(03)00071-3)
- Triantafyllidis P, Suhadolc P, Hatzidimitriou PM, Anastasiadis A, Theodulidis N (2004a) Part I. Theoretical site response estimation for microzoning purposes. *Pure Appl Geophys* 161:1185–1203. doi:[10.1007/s00024-003-2493-y](https://doi.org/10.1007/s00024-003-2493-y)
- Triantafyllidis P, Hatzidimitriou PM, Suhadolc P, Theodulidis N, Anastasiadis A (2004b) Part II. Comparison of theoretical and experimental estimations of site effects. *Pure Appl Geophys* 161:1205–1219. doi:[10.1007/s00024-003-2494-x](https://doi.org/10.1007/s00024-003-2494-x)